

SeeU: Seeing the Unseen World via 4D Dynamics-aware Generation

Yu Yuan¹, Tharindu Wickremasinghe¹, Zeeshan Nadir², Xijun Wang¹, Yiheng Chi¹, Stanley H. Chan¹
¹Purdue University ²Samsung Research America

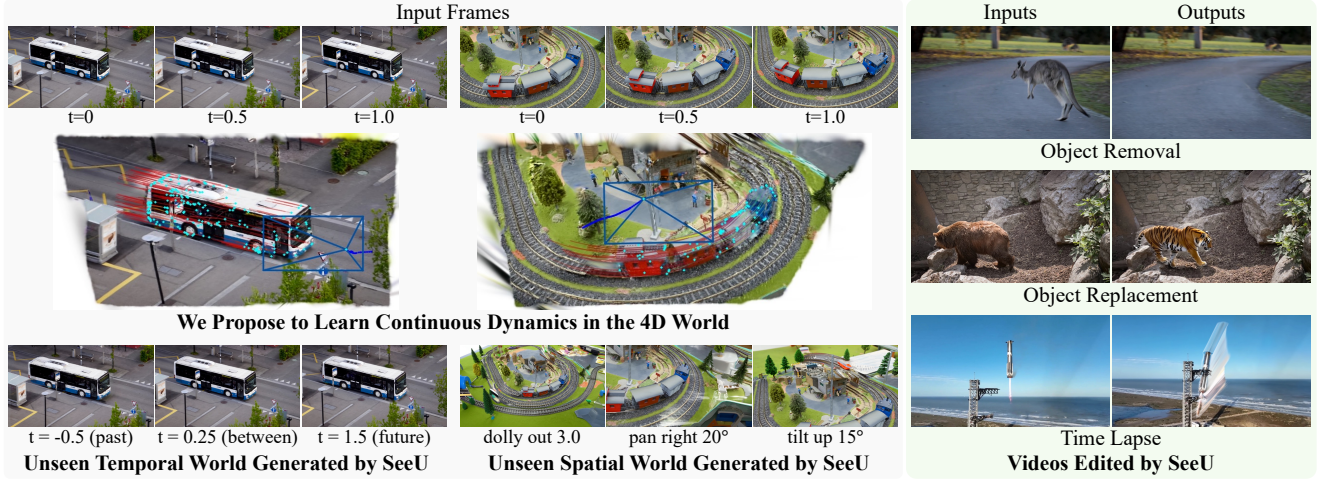


Figure 1. From sparse 2D frames, we learn vanilla and continuous 4D dynamics to better understand scenes and generate unseen worlds across novel times and viewpoints, while enforcing physically plausible motion and consistent 3D geometry.

Abstract

Images and videos are discrete 2D projections of the 4D world (3D space + time). Most visual understanding, prediction, and generation operate directly on 2D observations, leading to suboptimal performance. We propose **SeeU**, a novel approach that learns the continuous 4D dynamics and generate the unseen visual contents. The principle behind **SeeU** is a new **2D**→**4D**→**2D** learning framework. **SeeU** first reconstructs the 4D world from sparse and monocular 2D frames (**2D**→**4D**). It then learns the continuous 4D dynamics on a low-rank representation and physical constraints (discrete **4D**→continuous **4D**). Finally, **SeeU** rolls the world forward in time, re-projects it back to 2D at sampled times and viewpoints, and generates unseen regions based on spatial-temporal context awareness (**4D**→**2D**). By modeling dynamics in 4D, **SeeU** achieves continuous and physically-consistent novel visual generation, demonstrating strong potentials in multiple tasks including unseen temporal generation, unseen spatial generation, and video editing. All data and code will be public at [here](#).

1. Introduction

Humans live in a continuous four-dimensional (4D) space-time and have an exceptional ability to anticipate and imagine environmental evolution. This ability originates from spatial perception [9], intuitive physics understanding [5, 27], and brain mechanism that reconstructs memories to simulate the future [79]. A central challenge in machine vision is to endow artificial systems with human-like abilities to perceive, reason about, and generate the dynamic visual world from sensory observations.

To achieve this goal, end-to-end approaches attempt to model dynamics directly from 2D observations. Most methods operate in the pixel domain, learning temporal evolution from large-scale video data, and achieves strong results in video generation [10, 35, 43, 69, 70, 72, 87, 111], frame interpolation and prediction [22, 32, 59, 76, 81, 94, 121, 122, 124] and physics-aware generation [15, 68, 71, 80, 83, 104, 114]. Recent works learn dynamics in low-dimensional latent spaces [2, 41, 125], which greatly improves computational efficiency. However, these approaches have limitations:

1. The observed images and videos are discrete 2D projections of the 4D world onto the camera, directly modeling the dynamics leads to losses of important 3D structures

and temporal correlations.

2. The observations involve a combination of camera motion and scene dynamics, where the constantly changing camera pose increases the complexity and irregularity of scene motion.

As a result, models trained only on 2D visual patterns without effective 3D or physical supervision often fail to capture the underlying 3D geometry and physical dynamics of the scene. This limitation is more severe in complex out-of-distribution scenarios, such as occlusion, nonrigid deformation, and cluttered 2D projection trajectories.

To address these challenges, we propose to model the continuous 4D dynamics and understand the scenes before visual generation. We present a novel framework, **SeeU**, that performs visual understanding and generation, embodying this **2D→4D→2D** paradigm. The motivation behind this innovation is discussed in Section 2. SeeU is a departure from existing visual generation methods which focus on dynamics in the projected and discrete camera-only space. In SeeU, we first reconstruct a unified 4D representation with tracks from sparse monocular frames to explicitly disentangle camera, static background, and dynamic foreground (**2D→4D**). Next, continuous 4D dynamics of both the camera and the foreground are learned, producing efficient and physically consistent modeling of scene evolution (discrete **4D→continuous 4D**). Finally, with the learned dynamics, we interpolate/extrapolate to unseen times and viewpoints and re-project the 4D representation to 2D to obtain a video skeleton. A spatio-temporal in-context video generator then fills in appearance and details to produce the final video (**4D→2D**). By enforcing physically consistent 4D representations and dynamics, SeeU enables more interpretable and coherent understanding and generation of dynamic scenes.

We evaluate the proposed framework across a broad spectrum of vision tasks and settings, as illustrated in Fig. 1. In **unseen temporal** regimes, SeeU enables physically and spatially accurate past frame inference, dynamic frame interpolation, and future frame prediction. In **unseen spatial** regimes, SeeU synthesizes content for novel camera poses and previously occluded regions, maintaining geometric fidelity and semantic coherence across frames. SeeU also enables **video editing** applications, including object removal, object replacement, and time-lapse generation, demonstrating versatility and robustness.

In summary, we offer two contributions:

1. We introduce a novel concept SeeU, which allows us to see the unseen world through learning the continuous 4D dynamics from the 2D projections. We demonstrate the applicability of SeeU across unseen temporal generation, unseen spatial generation, and video editing.
2. The core innovation behind SeeU is a new **2D→4D→2D** learning framework that allows us to take 2D inputs and learn the 4D dynamics, and generate the required 2D

content. To our knowledge, this flow of information and the corresponding learning scheme is new in the literature.

2. Why Model Continuous Dynamics in 4D?

As illustrated in Fig. 2, projecting the continuous 4D world onto 2D images causes substantial loss of geometric and temporal information. This projection distorts spatial relationships, compresses motion signals, and weakens the physical regularities that govern the observed trajectories. Modeling continuous dynamics directly in the native 4D world has the following advantages:

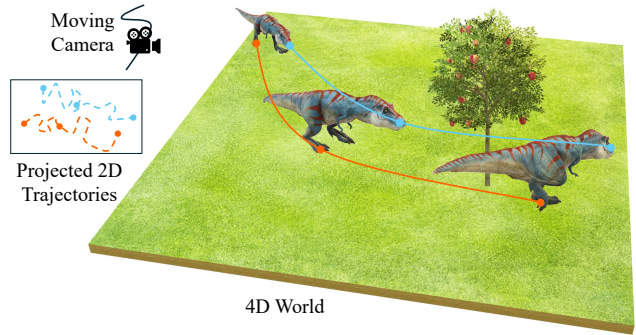


Figure 2. Projection and the entanglement of camera and scene motions make recovering accurate 3D geometry and physical trajectories directly from 2D frames particularly challenging; however, these quantities can usually be described in the 4D world explicitly, easily, and elegantly.

(i) 3D Awareness. Most perception and prediction methods are trained directly on large-scale 2D image/video data. Although they can perform interpolation and future frame prediction to some extent, they struggle in scenarios that require precise 3D reasoning, such as handling geometry, occlusions (see Fig. 4(b)), and viewpoint changes. The core limitation is the absence of an explicit 3D representation.

(ii) Physical Consistency. The **4D→2D** projection removes depth and structural cues and compresses temporal details, making the recovery of true motions from 2D pixel coordinates an ill-posed inverse problem (see the projected 2D trajectories shown in Fig. 2). In practice, many motions are simpler and more structured in 4D, governed by biological or mechanical constraints, classical mechanics, and energy or symmetry principles. These priors can be naturally expressed and learned in 4D. Moreover, casting dynamics as a continuous process in 4D naturally supports interpolation and extrapolation at arbitrary timestamps, leveraging physical priors to produce temporally coherent predictions.

(iii) Motion Disentanglement. When both the camera and the scene are in motion, modeling the dynamics in 2D becomes more difficult because each frame is captured from

a different pose where a stable observation coordinate system does not exist. In our framework, the camera, foreground, and background are represented in a unified 4D coordinate system, where their components are explicitly disentangled. Continuous dynamics are then modeled separately for the moving foreground and the camera.

3. Related Works

3.1. Dynamic Scene Representation

Dynamic NeRFs and 3D Gaussian Splatting. Neural radiance field (NeRF) [63] and 3D Gaussian Splatting (3DGS) [42] are the dominant backbones for 3D reconstruction and novel view synthesis. Recent works extend them to 4D by introducing additional time-dependent dynamics, such as a canonical 3D space with a learned deformation field [12, 48, 50, 89, 97, 100, 109, 110, 117]. These methods often require a noticeable camera parallax to provide multi-view constraints and tend to struggle when the foreground motion is large [25]. Shape-of-Motion [93] relaxes these assumptions by injecting depth and 2D tracking priors, improving performance under weaker parallax and faster motion.

Nonetheless, a common limitation remains for these methods under real-world monocular and temporally sparse inputs: the lack of continuous dynamics modeling leads to poor temporal extrapolation and interpolation (temporally unseen), and causes holes in reconstructions for previously unseen regions (spatially unseen).

Dense 3D Point Tracking. This emerging class of dynamic scene representation methods tracks dense 2D pixels across frames and back-projects them into 3D using multi-view consistency or depth priors, producing a time-varying 3D point cloud or mesh proxy [7, 23, 44, 58, 66, 67, 88, 92, 101, 102]. Such approaches provide explicit temporal correspondences.

However, their reconstructions are often sparse, noisy, and view-dependent, which limits temporal stability, spatial density, and reliable rendering from novel viewpoints.

3.2. Dynamics Modeling

Methods for modeling scene dynamics from videos can be broadly categorized into two types depending on whether the dynamics are learned implicitly or explicitly.

Implicit (End-to-End) Dynamics Learning. Most existing approaches learn dynamics directly from visual sequences in an end-to-end, data-driven manner. They are typically trained on large-scale video datasets using high-capacity sequence models such as Transformers [21, 86], multi-layer perceptrons (MLPs) [84] or state-space models (e.g., Mamba [30]). These methods implicitly capture motion and causal structure either in pixel space by learning frame-by-frame temporal evolution, or in a compact latent space, which improves efficiency. They have

demonstrated strong performance across a wide range of tasks, including world modeling [2, 41, 125], video generation [10, 35, 43, 69, 70, 72, 87, 111], frame interpolation and prediction [22, 32, 59, 76, 81, 94, 121, 122, 124], and physics-aware generation [15, 68, 71, 80, 83, 104, 114].

Explicit (Physics-Informed) Dynamics Learning. In contrast, physics-informed approaches incorporate explicit physical constraints into the learning process. They embed physical formalisms, such as Hamiltonian or Lagrangian dynamics [18, 29, 60, 123], into models to infer physical parameters or governing equations directly from videos [6, 14, 26, 28, 34, 37, 46, 49, 74, 95, 98, 99]. By enforcing physical consistency, these methods can perform tasks such as future frame prediction and physical parameter estimation, often requiring less data than data-driven approaches.

Despite their success, both categories are fundamentally limited to the 2D domain. After projection to the image plane, much of the true 3D geometry and temporal details is lost, and camera motion becomes entangled with scene dynamics. As a result, these approaches struggle to learn accurate and physically grounded dynamics of the real world.

3.3. Physics-aware Visual Generation

Diffusion models [33, 82] enable high-quality image synthesis [75, 77] and have been extended to video, where large-scale generative models learn motion from Internet-scale datasets [10, 35, 43, 69, 70, 87, 111]. Transformer-based diffusion architectures such as DiT [72] further improve scalability [40] and support powerful systems (e.g., Sora [70]). However, simply scaling these models up without effective physical embeddings leads to generated motions that may look plausible but break the real-world dynamics when out-of-distribution [3, 4, 15, 31, 39, 47, 55, 56, 62, 64, 115].

To improve physical consistency, recent work introduces physical priors into the generation process. They can be classified into three types. (1) Generation then Physical Simulation: A generator first produces static content and then a physics simulator animates it into videos [36, 54, 83, 103, 119]. This approach is interpretable and controllable, but requires intensive manual setup. (2) Physical Simulation then Generation: Simulate first to produce trajectories or constraints and then guide a video generator [16, 53, 57, 78, 104, 112]. The generator does not learn physics and is dependent on hand-specified rules. (3) Generation with Learned Physics Priors: physical cues are distilled from pretrained models and used to steer the generator directly [13, 15, 24, 51, 61, 71, 91, 105, 106, 108, 113, 114, 116, 120].

Different from above approaches, SeeU first infers deterministic dynamics from multi-frame observations, forming a physically coherent backbone for video generation.

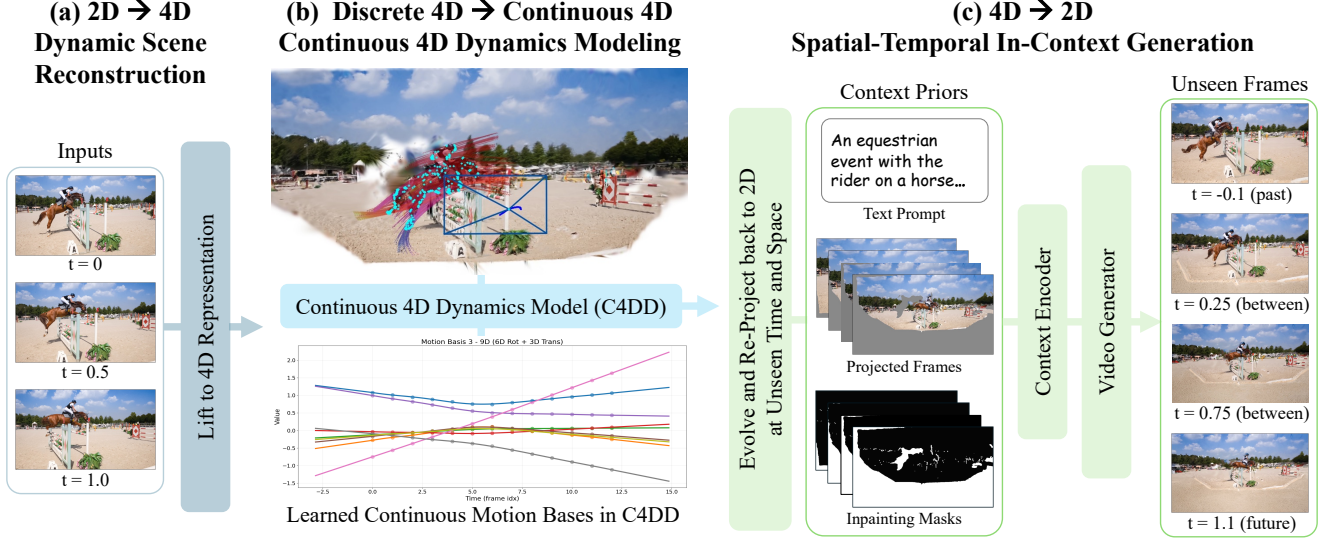


Figure 3. **Pipeline of SeeU.** (a) A dynamic scene is lifted into a 4D representation. (b) Continuous 4D dynamics are learned efficiently with physical and smoothness priors. (c) The learned dynamics evolve the 4D world, which is re-projected to 2D at unseen times and viewpoints; a spatial-temporal in-context video generator completes the unobserved or uncertain areas.

4. Proposed Methods

4.1. Problem Definition and Overview

Given a monocular frame sequence $\{I_t \in \mathbb{R}^{H \times W \times 3}\}$ of a dynamic scene, SeeU aims to synthesize novel content at unobserved times and viewpoints beyond the input frames.

SeeU follows a three-stage pipeline (Fig. 3): (i) 2D→4D, (ii) Discrete 4D→Continuous 4D, and (iii) 4D→2D.

4.2. Dynamic Scene Reconstruction (2D→4D)

In the first stage, SeeU reconstructs the dynamic 4D world with motion trajectories (both dynamic foreground and camera) across time. Our method builds on Shape-of-Motion [93] for two specific reasons: (1) it is compatible with casual inputs with limited parallax, and (2) explicitly separates static regions from trackable dynamic elements.

We represent the dynamic scene with a set of canonical 3D Gaussians $\{g_0^i\}_{i=1}^N$ that persist over time. Each canonical Gaussian is parameterized as

$$g_0^i = (\mu_0^i, \mathbf{R}_0^i, \mathbf{s}^i, o^i, \mathbf{c}^i), \quad (1)$$

where $\mu_0^i \in \mathbb{R}^3$ denotes the canonical mean, $\mathbf{R}_0^i \in \mathbb{SO}(3)$ the canonical orientation, $\mathbf{s}^i \in \mathbb{R}^3$ the scale, $o^i \in \mathbb{R}$ the opacity, and $\mathbf{c}^i \in \mathbb{R}^3$ the color. To model changes, each Gaussian evolves from the canonical frame t_0 to frame t via a per-frame rigid transformation $\mathbf{T}_{0 \rightarrow t} = [\mathbf{R}_{0 \rightarrow t}, \mathbf{t}_{0 \rightarrow t}] \in \mathbb{SE}(3)$:

$$\mu_t^i = \mathbf{R}_{0 \rightarrow t} \mu_0^i + \mathbf{t}_{0 \rightarrow t}, \quad \mathbf{R}_t^i = \mathbf{R}_{0 \rightarrow t} \mathbf{R}_0^i. \quad (2)$$

Specifically, for the input frames I_t , we first estimate the camera intrinsics, extrinsics, and per-frame depth using

MegaSAM [52]. We then obtain segmentation masks of moving foreground objects with Track-Anything [107], and extract 2D point tracks using TAPIR [20]. Finally, we fuse the RGB frames with these 2D priors to infer a dynamic scene representation, and output the frame-level camera pose and attributes of each foreground Gaussian properties \mathbf{P} (e.g., position, orientation, and scale).

4.3. Continuous 4D Dynamics Modeling (Discrete 4D→Continuous 4D)

With the frame-level camera poses and the per-frame attributes of each foreground Gaussian obtained from Stage 1, our goal is to recover physically credible, continuous-time 4D dynamics from these discrete observations. Let \mathbf{P}_t^i denote the attributes of the i -th Gaussian at frame t , and let \mathbf{C}_t be the camera pose at frame t . We seek continuous trajectories for the Gaussians and the camera.

This task presents two main challenges: (1) **Efficiency**. The number of foreground Gaussians can be large (e.g., 80k), making it infeasible to learn an independent time-varying trajectory for each primitive. (2) **Physical Consistency**. The recovered trajectories should be smooth and physically plausible, avoiding abrupt, nonphysical jumps in position, rotation, velocity, or acceleration.

To address challenge (1), we employ a low-rank motion parameterization inspired by Shape-of-Motion [93]. For any foreground Gaussian i at time t , its properties \mathbf{P}_t^i are

$$\mathbf{P}_t^i = \mathbf{P}_0^i + \underbrace{\mathbf{B}(t)}_{\in \mathbb{R}^{m \times K}} \underbrace{\mathbf{w}_i}_{\in \mathbb{R}^K}, \quad \mathbf{P}_0^i, \mathbf{P}_t^i \in \mathbb{R}^m. \quad (3)$$

where \mathbf{P}_0^i is the initial state of Gaussian i , $\mathbf{B}(t)$ is a set of global motion basis functions shared by all Gaussians, and \mathbf{w}_i is a time-invariant coefficient vector for Gaussian i . Through this parameterization, instead of directly learning N separate trajectories, we learn only a small number K of shared basis functions $\mathbf{B}(t)$ (where $K \ll N$), and each Gaussian is represented by few coefficients. The discrete motion bases are first initialized from 3D point trajectories using Procrustes analysis, and subsequently refined by minimizing the photometric reconstruction error.

To address challenge (2), we observe that in natural sequences without sudden disturbances, both the per motion basis trajectory and the camera pose trajectory points in $\mathbb{SE}(3)$, exhibit simple and smooth temporal trends shown in Fig. 3(b), despite complex motions in raw videos. This motivates modeling them as continuous time functions parameterized by B-spline curves.

Motivated by the above analysis, we formulate a lightweight, physics-aware **Continuous 4D Dynamics Model (C4DD)** that explicitly learns the control points $\{\mathbf{q}_j\}_{j=1}^M$ of the B-spline functions

$$\hat{\mathbf{B}}_t = \sum_{j=1}^M N_{j,d}(t) \mathbf{q}_j, \quad (4)$$

where $\{N_{j,d}(t)\}$ are the B-spline basis functions and \mathbf{q}_j are the learnable control points for the motion bases. The number of control points M controls the curve capacity: larger M allows richer temporal variations, while smaller M enforces stronger smoothness and regularization.

During training, both the camera and the shared motion bases are optimized jointly under a hybrid objective:

$$\mathcal{L}_{\text{total}} = \underbrace{\mathcal{L}_{\text{data}}}_{\text{data loss}} + \lambda_{\text{phys}} \underbrace{\mathcal{L}_{\text{phys}}}_{\text{physical loss}}. \quad (5)$$

The data term enforces consistency between the C4DD-estimated motion bases and the discrete observations obtained in challenge (1):

$$\mathcal{L}_{\text{data}} = \sum_{t \in \mathcal{T}_{\text{obs}}} \|\hat{\mathbf{B}}_t - \mathbf{B}_t^{\text{obs}}\|_2^2, \quad (6)$$

where $\mathbf{B}_t^{\text{obs}}$ denotes the observed (discrete) motion bases at timestamp t , and $\hat{\mathbf{B}}_t$ is the C4DD prediction evaluated from the B-spline parameterization:

To further enforce physical plausibility, we regularize the temporal derivatives of both the motion bases and the camera trajectories. The physical loss penalizes rapid changes in translation and rotation, with larger weights assigned to extrapolated time intervals:

$$\mathcal{L}_{\text{phys}} = \mathbb{E}_{\tau_{\text{ex}}(t)} \left[\|\ddot{\mathbf{M}}\mathbf{B}_{\text{trans}}(t)\|_2^2 + \|\ddot{\mathbf{C}}\mathbf{a}\mathbf{m}_{\text{trans}}(t)\|_2^2 + \mathbb{I}_{\text{rot}} \|\ddot{\mathbf{C}}\mathbf{a}\mathbf{m}_{\text{rot}}(t)\|_2^2 \right], \quad (7)$$

where $\ddot{\mathbf{M}}\mathbf{B}_{\text{trans}}(t)$ and $\ddot{\mathbf{C}}\mathbf{a}\mathbf{m}_{\text{trans}}(t)$ denote the second-order temporal derivatives of the translational components for the motion bases and the camera trajectory, respectively; $\ddot{\mathbf{C}}\mathbf{a}\mathbf{m}_{\text{rot}}(t)$ is the rotational acceleration; $\mathbb{I}_{\text{rot}} \in \{0, 1\}$ toggles rotation regularization; $\tau_{\text{ex}}(t)$ assigns higher weights to unobserved (extrapolated) time spans in the past or future.

4.4. Spatial-Temporal In-Context Generation (4D→2D)

Leveraging the continuous 4D dynamics learned in Stage 2 together with the Stage 1 scene representation, we evolve the scene to any timestamp. We then either position the camera at a desired pose or evolve its pose via C4DD and render the resulting 2D projection, which acts as a video scaffold encoding precise geometry, motion, and occlusion structure.

Note that the scaffold may be incomplete, as certain regions can be missing or unreliable, including: (1) areas never observed (novel viewpoints or previously occluded regions), (2) locations where the projected Gaussians yield low confidence, and (3) thin structures and sharp depth discontinuities that can introduce projection artifacts (e.g., along object boundaries and occlusion edges).

To address these issues, we leverage the strong spatial-temporal in-context capabilities [8, 38, 96] of video generation models to repair frames (Fig. 3(c)). We supply the model with three types of context priors: (1) a structured prompt derived from a vision-language model (VLM) [90] as a caption of the scene, which encodes global semantics, and specifies the inpainting content, (2) projected frames that serve as a geometric and photometric reference, and (3) per-frame inpainting masks detected during projection that mark uncertain or missing regions. A Context Encoder ingests these priors, produces context embeddings, and injects them into a pre-trained video generator. With these context priors, the video generator fills in high-frequency details, textures, and temporal coherent contents in regions uncertain or unseen in the original observations.

5. Experiments

We evaluate SeeU in novel content generation tasks where major challenges originate from *unseen time* (e.g., past, between-frames, and future) and *unseen space* (e.g., camera motion and occlusion). We also demonstrate its broader potential in video editing. Section 5.1 presents implementation details, Section 5.2 compares SeeU with other baselines, Section 5.3 discusses ablation results, and Section 5.4 focuses on video editing applications.

5.1. Implementation Details

Datasets. We evaluate our framework on SEEU45, a curated set of 45 dynamic scenes assembled from our own captures and public sources, including video tracking dataset TAP-vid [19, 73], high frame-rate I2-2000FPS [17], robotics video set

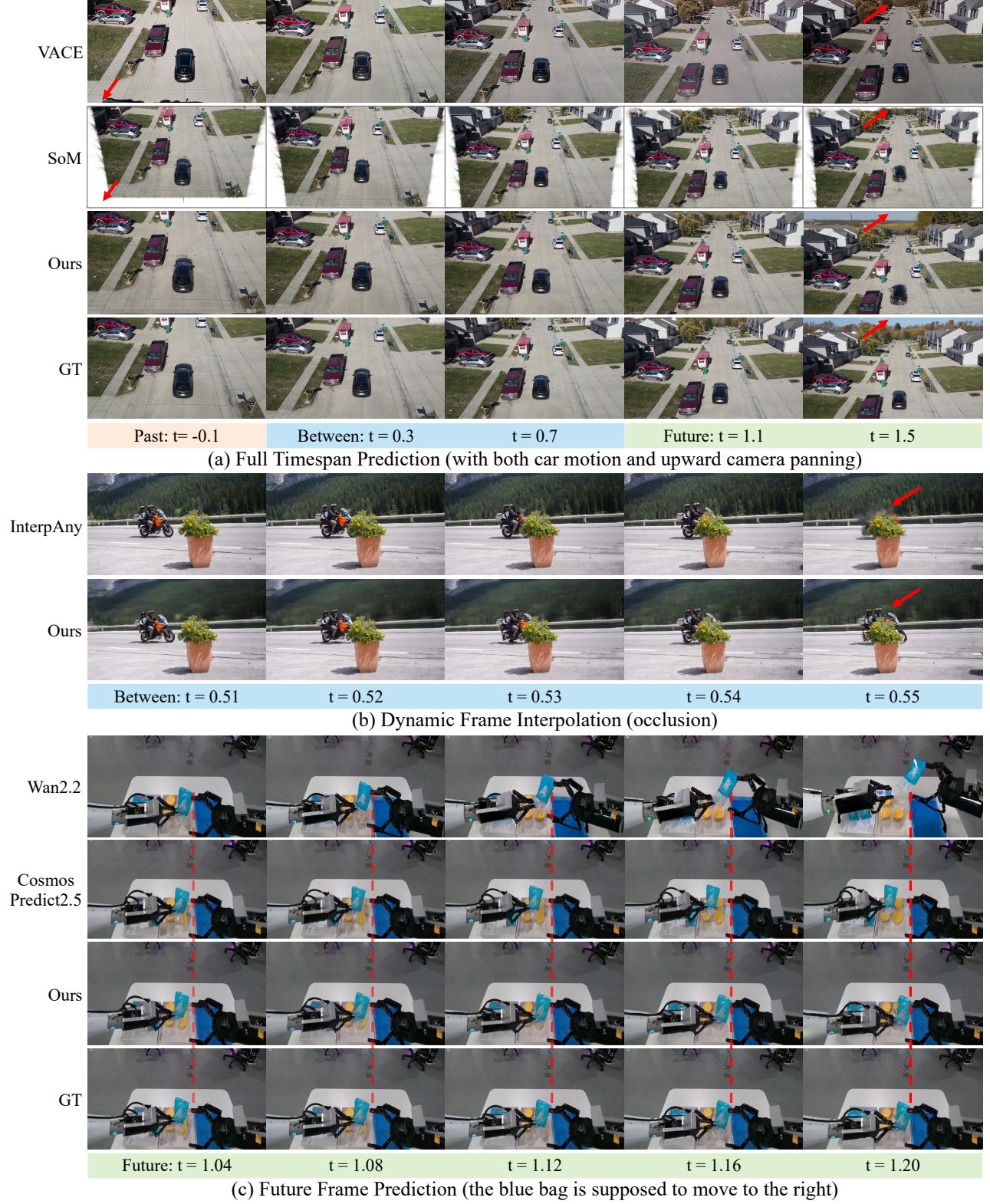


Figure 4. **Visual comparisons on unseen temporal generation.** SeeU supports continuous-time generation across the entire time span (**past** – **between** – **future**), yielding more physically plausible motion and stronger geometric consistency.

Methods	Past (6.67%) Frame Inference				Dynamic Frame Interpolation				Future (6.67%) Frame Prediction			
	PSNR \uparrow	SSIM \uparrow	LPIPS \downarrow	C-LPIPS	PSNR \uparrow	SSIM \uparrow	LPIPS \downarrow	C-LPIPS	PSNR \uparrow	SSIM \uparrow	LPIPS \downarrow	C-LPIPS
Reference	—	—	—	0.0397	—	—	—	0.0356	—	—	—	0.0389
InterpAny [124]	—	—	—	—	20.5406	0.5636	0.2420	0.0525	—	—	—	—
Wan 2.2 [87]	—	—	—	—	—	—	—	—	18.2989	0.5064	0.2559	0.0704
Cosmos [69]	—	—	—	—	—	—	—	—	20.0672	0.5557	0.2885	0.0355
SoM [93]	15.5464	0.4518	0.3876	0.0116	16.3650	0.4814	0.3555	0.0340	15.4301	0.4585	0.3885	0.0141
VACE [38]	17.1430	0.4648	0.3673	0.0924	18.1617	0.5041	0.3587	0.1821	17.7080	0.4938	0.3543	0.1244
Ours	20.4682	0.5496	0.2484	0.0355	21.0726	0.5715	0.2271	0.0327	20.5353	0.5581	0.2431	0.0358

Table 1. **Quantitative comparison on unseen temporal generation.** Metrics are averaged across all scenes. The extrapolation windows (past and future) each covers 6.67% of the sequence duration. Best values are shown in **bold**. Note that C-LPIPS is not lower-better; it should be close to the reference value.

Methods	Dolly Out			Dolly Right			Dolly Up			Tilt Up			Pan Right		
	EE \downarrow	EIR \uparrow	CLIP-V \uparrow	EE \downarrow	EIR \uparrow	CLIP-V \uparrow	EE \downarrow	EIR \uparrow	CLIP-V \uparrow	EE \downarrow	EIR \uparrow	CLIP-V \uparrow	EE \downarrow	EIR \uparrow	CLIP-V \uparrow
GCD [85]	0.2004	0.5129	0.9253	—	—	—	—	—	—	—	—	—	—	—	—
ReCamMaster [1]	0.2382	0.6736	0.9366	0.2130	0.7049	0.9227	0.2087	0.7053	0.9248	0.2281	0.7161	0.9256	0.2146	0.7035	0.9250
Ours	0.1997	0.7848	0.9690	0.1895	0.7947	0.9542	0.1908	0.7841	0.9695	0.2082	0.8208	0.9466	0.1891	0.8229	0.9574

Table 2. **Quantitative comparison on unseen spatial generation.** Lower Epipolar Error (EE) and higher Epipolar Inlier Ratio (EIR) indicate better 3D geometric consistency, and higher CLIP-V refers to higher scene consistency.

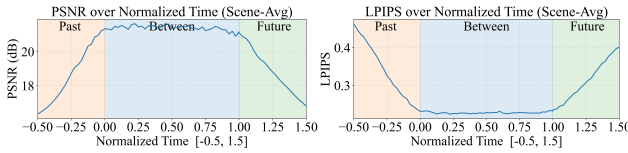


Figure 5. **Temporal prediction error analysis.**

Methods	Unseen Temporal			Unseen Spatial	
	PSNR \uparrow	SSIM \uparrow	LPIPS \downarrow	EE \downarrow	CLIP-V \uparrow
C4DD w/ MLP	17.5372	0.3934	0.4274	0.3125	0.7390
w/o physics loss	19.3593	0.5274	0.2735	0.2240	0.9198
Ours (5 frames)	18.3583	0.4521	0.3054	0.2852	0.9284
Ours (10 frames)	20.1626	0.5378	0.2507	0.2044	0.9551
Ours (15 frames)	20.3870	0.5484	0.2408	0.2003	0.9581
Ours (20 frames)	21.0832	0.5522	0.2387	0.1972	0.9596

Table 3. **Quantitative results of ablation study.**

AgiBot World [11], and Animal Kingdom dataset [65]. The collection of scenes spans indoor/outdoor environments, diverse subjects (animals, robots, humans, everyday objects), and a wide range of camera regimes (static, handheld) and motion types (rigid/non-rigid).

Training Details. SeeU is trained and run in three stages sequentially. All stages are trained with Adam optimizer on a single NVIDIA A100 (80 GB) GPU. In the first stage (2D \rightarrow 4D), the numbers of Gaussian primitives are 80,000 for the dynamic foreground and 80,000 for the background, and 10 motion bases are learned. The learnable components are optimized for 4,000 iterations. For a typical 10-frame sequence of 960×540 resolution, this optimization takes approximately 1 hour. In the second stage (Discrete 4D \rightarrow Continuous 4D), we train the Contin-

uous 4D Dynamics Model (C4DD) using cubic (deg = 3) B-splines with 8 control points and a physics loss weight of $\lambda_{\text{phy}} = 1 \times 10^{-4}$. The learning rate is 1×10^{-5} , and the batch size is 64. Training 1,000 epochs takes ~ 10 minutes. In the third stage (4D \rightarrow 2D), we perform a computationally efficient fine-tuning of VACE [38] on our multi-semantic-mask distribution, which takes approximately 2 hours.

Metrics. For unseen time, we evaluate physical accuracy and frame-to-frame consistency, and, for unseen space, 3D geometry and scene-level coherence. To evaluate temporally unseen generation, we sample a subset of intermediate frames per scene as input and generate their (i) past, (ii) in-between, and (iii) future frames. We compare the generation results with their temporally nearest frames in the full sequence, reporting PSNR, SSIM, LPIPS [118], and cross-frame consistency C-LPIPS [113]. To evaluate spatially unseen generation, we measure (i) 3D geometric agreement using Epipolar Error (EE) and Epipolar Inlier Ratio (EIR) (details in Suppl. Materials) and (ii) semantic consistency between source and target frames using CLIP-V [45].

5.2. Results

Temporally Unseen Generation. We evaluate performance on three sub-tasks: past frame inference, dynamics frame interpolation (between-frames), and future frame prediction. As currently no single baseline can comprehensively address all three tasks, we benchmark SeeU against a suite of specialized state-of-the-art (SOTA) methods, including video frame interpolation model InterpAny [124], future predictor COSMOS Predict2.5 [69], and image-to-video generator Wan2.2 [87] conditioned on the last frame. In addition, we extend VACE [38] to cover the full temporal range by

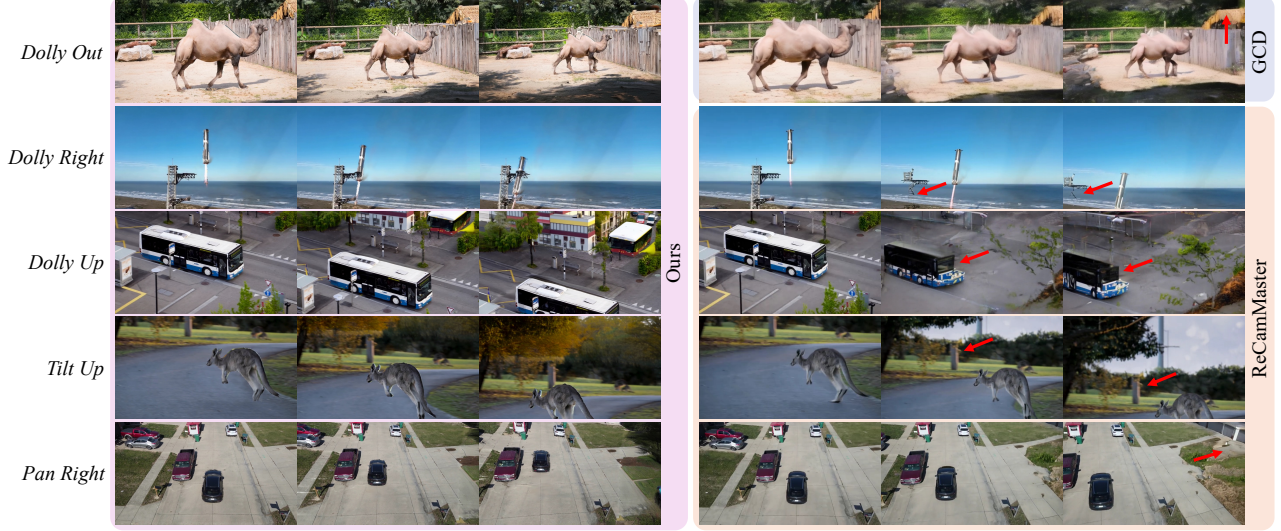


Figure 6. **Visual comparisons on unseen spatial generation.** SeeU exhibits strong 3D awareness and scene consistency.

masking unseen frames, and Shape-of-Motion [93] by performing linear interpolation and extrapolation. As shown in Fig. 4 and Table 1, SeeU demonstrates stronger continuous-time dynamics awareness and 3D geometric interpretation, outperforming baselines in temporal extrapolation and dynamic interpolation with more physically plausible motion and higher geometric consistency. Fig. 5 presents the temporal prediction error analysis over the time span from the past 50% to the future 50%. We observe a decrease of accuracy in the extrapolated regions approximately linear to the temporal distance.

Spatially Unseen Generation. We compare SeeU with specialized camera-controllable video models GCD [85] and ReCamMaster [1]. The evaluation is performed by experimenting on five canonical camera motions: *dolly-out*, *dolly-right*, *dolly-up*, *tilt-up*, and *pan-right*. As illustrated in Fig. 6, SeeU produces temporally smoother results, providing more coherent visual continuity and generating more accurate spatial occlusions. Table 2 demonstrates that SeeU achieves higher geometric fidelity (EE and EIR) and scene consistency (CLIP-V) than all baselines, reflecting its capability to render richer scene details.

5.3. Ablation Study

C4DD Architecture. We replace the B-spline parameterization with plain MLP layers. Tabel 3 indicates that this variant produces results with reduced temporal smoothness and physical consistency, confirming the advantageous inductive bias of spline priors for continuous dynamics.

Physics-Informed Loss. Table 3 shows that setting the physics loss weight λ_{phy} to 0 degrades frame consistency, highlighting the role of physics constraints in stabilizing continuous dynamics.

Input Sparsity. As shown in Table. 3, we investigate the effects of sparse observations by subsampling the input to 5/10/15/20 frames. C4DD maintains stable performance as frame density decreases, demonstrating robustness to sparse inputs and preservation of temporal continuity.

5.4. Application to Video Editing

By constructing a continuous, unified model of time and 3D space, SeeU enables a variety of video editing applications, as shown in Fig. 1. For example, **object removal** can be performed by deleting foreground Gaussians and inpainting the revealed background regions by de-occlusion. By replacing the original foreground content and conditioning on a new text prompt, SeeU also enables controllable **object replacement** in videos. Leveraging the learned continuous 4D dynamics, we can further re-parameterize foreground trajectories in time to create **time-lapse** effects.

6. Conclusions

SeeU implements a $2D \rightarrow 4D \rightarrow 2D$ pathway to achieve a unified understanding and generation. The technical core of SeeU is the construction of physically-consistent, continuous 4D dynamics within the native 4D world to describe its dynamic evolution. Combined with in-context video generation, SeeU synthesizes previously unseen content across time and space, enabling advances in world modeling and narrowing the gap between physical and generative domains.

Limitation: SeeU is applicable to a broad range of real-world dynamic scenes; however, given the limitations of the underlying modules (tracking, camera estimation, and 4D reconstruction), this paper focuses on inputs with pronounced, smooth, and temporally stable foreground motion.

Acknowledgments

This work is supported, in part, by the United States National Science Foundation under the grants 2133032, 2431505, and a research award from Samsung Research America.

We thank Yichen Sheng and Lu Ning for helpful discussion.

References

- [1] Jianhong Bai, Menghan Xia, Xiao Fu, Xintao Wang, Lianrui Mu, Jinwen Cao, ZuoZhu Liu, Haoji Hu, Xiang Bai, Pengfei Wan, et al. ReCamMaster: Camera-controlled generative rendering from a single video. In *International Conference on Computer Vision*, 2025. 7, 8
- [2] Federico Baldassarre, Marc Szafraniec, Basile Terver, Vasil Khalidov, Francisco Massa, Yann LeCun, Patrick Labatut, Maximilian Seitzera, and Piotr Bojanowski. Back to the features: Dino as a foundation for video world models. *arXiv preprint arXiv: 2507.19468*, 2025. 1, 3
- [3] Hritik Bansal, Zongyu Lin, Tianyi Xie, Zeshun Zong, Michal Yarom, Yonatan Bitton, Chenfanfu Jiang, Yizhou Sun, Kai-Wei Chang, and Aditya Grover. VideoPhy: Evaluating physical commonsense for video generation. *arXiv preprint arXiv:2406.03520*, 2024. 3
- [4] Hritik Bansal, Clark Peng, Yonatan Bitton, Roman Gold-berg, Aditya Grover, and Kai-Wei Chang. VideoPhy-2: A challenging action-centric physical commonsense evaluation in video generation. *arXiv preprint arXiv:2503.06800*, 2025. 3
- [5] Adrien Bardes, Quentin Garrido, Jean Ponce, Michael Rabbat, Yann LeCun, Mahmoud Assran, and Nicolas Ballas. Revisiting feature prediction for learning visual representations from video. *arXiv:2404.08471*, 2024. 1
- [6] Filipe de Avila Belbute-Peres, Kevin Smith, Kelsey Allen, and Josh Tenenbaum. End-to-end differentiable physics for learning and control. In *Advances in Neural Information Processing Systems*, 2018. 3
- [7] Weikang Bian, Zhaoyang Huang, Xiaoyu Shi, Yijin Li, Fu-Yun Wang, and Hongsheng Li. Gs-dit: Advancing video generation with dynamic 3d gaussian fields through efficient dense 3d point tracking. In *IEEE/CVF Conference on Computer Vision and Pattern Recognition*, 2025. 3
- [8] Yuxuan Bian, Zhaoyang Zhang, Xuan Ju, Mingdeng Cao, Liangbin Xie, Ying Shan, and Qiang Xu. Videopainter: Any-length video inpainting and editing with plug-and-play context control. In *SIGGRAPH*, 2025. 5
- [9] Irving Biederman. Perceiving real-world scenes. *Science*, 1972. 1
- [10] Andreas Blattmann, Tim Dockhorn, Sumith Kulal, Daniel Mendelevitch, Maciej Kilian, Dominik Lorenz, Yam Levi, Zion English, Vikram Voleti, Adam Letts, Varun Jampani, and Robin Rombach. Stable video diffusion: Scaling latent video diffusion models to large datasets. *arXiv preprint arXiv:2311.15127*, 2023. 1, 3
- [11] Qingwen Bu, Jisong Cai, Li Chen, Xiuqi Cui, Yan Ding, Siyuan Feng, Xindong He, Xu Huang, et al. Agibot world colosseum: A large-scale manipulation platform for scalable and intelligent embodied systems. In *International Conference on Intelligent Robots and Systems*, 2025. 7, 1
- [12] Ang Cao and Justin Johnson. HexPlane: A fast representation for dynamic scenes. *IEEE/CVF Conference on Computer Vision and Pattern Recognition*, 2023. 3
- [13] Qinglong Cao, Ding Wang, Xirui Li, Yuntian Chen, Chao Ma, and Xiaokang Yang. Teaching video diffusion model with latent physical phenomenon knowledge. *arXiv preprint arXiv:2411.11343*, 2024. 3
- [14] Pradyumna Chari, Chinmay Talegaonkar, Yunhao Ba, and Achuta Kadambi. Visual physics: Discovering physical laws from videos. *arXiv preprint arXiv:1911.11893*, 2019. 3
- [15] Hila Chefer, Uriel Singer, Amit Zohar, Yuval Kirstain, Adam Polyak, Yaniv Taigman, Lior Wolf, and Shelly Sheynin. VideoJAM: Joint appearance-motion representations for enhanced motion generation in video models. In *International Conference on Machine Learning*, 2025. 1, 3
- [16] Boyuan Chen, Hanxiao Jiang, Shaowei Liu, Saurabh Gupta, Yunzhu Li, Hao Zhao, and Shenlong Wang. PhysGen3D: Crafting a miniature interactive world from a single image. In *IEEE/CVF Conference on Computer Vision and Pattern Recognition*, 2025. 3
- [17] Prateek Chennuri, Yiheng Chi, Enze Jiang, GM Dilshan Godaliyadda, Abhiram Gnanasambandam, Hamid R Sheikh, Istvan Gyongy, and Stanley H Chan. Quanta video restoration. In *European Conference on Computer Vision*, 2024. 5, 1
- [18] Congyue Deng, Brandon Y. Feng, Cecilia Garraffo, Alan Garbarz, Robin Walters, William T. Freeman, Leonidas Guibas, and Kaiming He. Denoising hamiltonian network for physical reasoning. *arXiv preprint arXiv:2503.0759*, 2025. 3
- [19] Carl Doersch, Ankush Gupta, Larisa Markeeva, Adria Recasens, Lucas Smaira, Yusuf Aytar, Joao Carreira, Andrew Zisserman, and Yi Yang. TAP-Vid: A benchmark for tracking any point in a video. *Advances in Neural Information Processing Systems*, 2022. 5, 1
- [20] Carl Doersch, Yi Yang, Mel Vecerik, Dilara Gokay, Ankush Gupta, Yusuf Aytar, Joao Carreira, and Andrew Zisserman. TAPIR: Tracking any point with per-frame initialization and temporal refinement. In *International Conference on Computer Vision*, 2023. 4
- [21] Alexey Dosovitskiy, Lucas Beyer, Alexander Kolesnikov, Dirk Weissenborn, Xiaohua Zhai, Thomas Unterthiner, Mostafa Dehghani, Matthias Minderer, Georg Heigold, Sylvain Gelly, Jakob Uszkoreit, and Neil Houlsby. An image is worth 16x16 words: Transformers for image recognition at scale. *International Conference on Learning Representations*, 2021. 3
- [22] Haiwen Feng, Zheng Ding, Zhihao Xia, Simon Niklaus, Victoria Abrevaya, Michael J. Black, and Xuaner Zhang. Explorative inbetweening of time and space. In *European Conference on Computer Vision*, 2024. 1, 3
- [23] Haiwen Feng*, Junyi Zhang*, Qianqian Wang, Yufei Ye, Pengcheng Yu, Michael J. Black, Trevor Darrell, and Angjoo Kanazawa. St4RTrack: Simultaneous 4d reconstruction and tracking in the world. In *International Conference on Computer Vision*, 2025. 3

- [24] Tao Feng, Xianbing Zhao, Zhenhua Chen, Tien Tsin Wong, Hamid Rezaatofighi, Gholamreza Haffari, and Lizhen Qu. Physics-grounded motion forecasting via equation discovery for trajectory-guided image-to-video generation. *arXiv preprint arXiv:2507.06830*, 2025. 3
- [25] Hang Gao, Ruilong Li, Shubham Tulsiani, Bryan Russell, and Angjoo Kanazawa. Dynamic novel-view synthesis: A reality check. In *Advances in Neural Information Processing Systems*, 2022. 3
- [26] Alejandro Castañeda Garcia, Jan van Gemert, Daan Brinks, and Nergis Tömen. Learning physics from video: Unsupervised physical parameter estimation for continuous dynamical systems. In *IEEE/CVF Conference on Computer Vision and Pattern Recognition*, 2025. 3
- [27] Quentin Garrido, Nicolas Ballas, Mahmoud Assran, Adrien Bardes, Laurent Najman, Michael Rabbat, Emmanuel Dupoux, and Yann LeCun. Intuitive physics understanding emerges from self-supervised pretraining on natural videos. *arXiv preprint arXiv: 2502.11831*, 2025. 1
- [28] Quentin Garrido, Nicolas Ballas, Mahmoud Assran, Adrien Bardes, Laurent Najman, Michael Rabbat, Emmanuel Dupoux, and Yann LeCun. Intuitive physics understanding emerges from self-supervised pretraining on natural videos. *arXiv preprint arXiv:2502.08987*, 2025. 3
- [29] Samuel Greydanus, Misko Dzamba, and Jason Yosinski. Hamiltonian neural networks. In *Advances in Neural Information Processing Systems*, 2019. 3
- [30] Albert Gu and Tri Dao. Mamba: Linear-time sequence modeling with selective state spaces. *arXiv preprint arXiv:2312.00752*, 2023. 3
- [31] Jing Gu, Xian Liu, Yu Zeng, Ashwin Nagarajan, Fangrui Zhu, Daniel Hong, Yue Fan, Qianqi Yan, Kaiwen Zhou, Ming-Yu Liu, and Xin Eric Wang. PhyWorldBench: A comprehensive evaluation of physical realism in text-to-video models. *arXiv preprint arXiv:2507.13428*, 2025. 3
- [32] Zujin Guo, Wei Li, and Chen Change Loy. Generalizable implicit motion modeling for video frame interpolation. In *Advances in Neural Information Processing Systems*, 2024. 1, 3
- [33] Jonathan Ho, Ajay Jain, and Pieter Abbeel. Denoising diffusion probabilistic models. In *Advances in Neural Information Processing Systems*, 2020. 3
- [34] Florian Hofherr, Lukas Koestler, Florian Bernard, and Daniel Cremers. Neural implicit representations for physical parameter inference from a single video. In *IEEE/CVF Winter Conference on Applications of Computer Vision*, 2023. 3
- [35] Wenyi Hong, Ming Ding, Wendi Zheng, Xinghan Liu, and Jie Tang. CogVideo: Large-scale pretraining for text-to-video generation via transformers. In *International Conference on Learning Representations*, 2023. 1, 3
- [36] Hao-Yu Hsu, Zhi-Hao Lin, Albert Zhai, Hongchi Xia, and Shenlong Wang. AutoVFX: Physically realistic video editing from natural language instructions. *arXiv preprint arXiv:2411.02394*, 2024. 3
- [37] Miguel Jaques, Michael Burke, and Timothy Hospedales. Physics-as-Inverse-Graphics: Unsupervised physical parameter estimation from video. In *International Conference on Learning Representations*, 2020. 3
- [38] Zeyinzi Jiang, Zhen Han, Chaojie Mao, Jingfeng Zhang, Yulin Pan, and Yu Liu. VACE: All-in-one video creation and editing. In *International Conference on Computer Vision*, 2025. 5, 7, 1
- [39] Bingyi Kang, Yang Yue, Rui Lu, Zhijie Lin, Yang Zhao, Kaixin Wang, Gao Huang, and Jiashi Feng. How far is video generation from world model: A physical law perspective. In *International Conference on Machine Learning*, 2025. 3
- [40] Jared Kaplan, Sam McCandlish, Tom Henighan, Tom B. Brown, Benjamin Chess, Rewon Child, Scott Gray, Alec Radford, Jeffrey Wu, and Dario Amodei. Scaling laws for neural language models. *arXiv preprint arXiv: 2001.08361*, 2020. 3
- [41] Efsthathios Karypidis, Ioannis Kakogeorgiou, Spyros Gidaris, and Nikos Komodakis. DINO-Foresight: Looking into the future with dino. In *Advances in Neural Information Processing Systems*, 2025. 1, 3
- [42] Bernhard Kerbl, Georgios Kopanas, Thomas Leimkühler, and George Drettakis. 3d gaussian splatting for real-time radiance field rendering. *ACM Transactions on Graphics*, 2023. 3
- [43] Weijie Kong, Qi Tian, Zijian Zhang, Rox Min, Zuozhuo Dai, Jin Zhou, Jiangfeng Xiong, Xin Li, Bo Wu, Jianwei Zhang, et al. Hunyuanvideo: A systematic framework for large video generative models. *arXiv preprint arXiv:2412.03603*, 2024. 1, 3
- [44] Skanda Koppula, Ignacio Rocco, Yi Yang, Joe Heyward, João Carreira, Andrew Zisserman, Gabriel Brostow, and Carl Doersch. Tapvid-3d: A benchmark for tracking any point in 3d. In *Advances in Neural Information Processing Systems*, 2024. 3
- [45] Zhengfei Kuang, Shengqu Cai, Hao He, Yinghao Xu, Hongsheng Li, Leonidas Guibas, and Gordon Wetzstein. Collaborative video diffusion: Consistent multi-video generation with camera control. In *arXiv preprint arXiv:2405.17414*, 2024. 7
- [46] Vincent Le Guen and Nicolas Thome. Disentangling physical dynamics from unknown factors for unsupervised video prediction. In *IEEE/CVF Conference on Computer Vision and Pattern Recognition*, 2020. 3
- [47] Chenyu Li, Oscar Michel, Xichen Pan, Sainan Liu, Mike Roberts, and Saining Xie. PISA experiments: Exploring physics post-training for video diffusion models by watching stuff drop. In *International Conference on Machine Learning*, 2025. 3
- [48] Jinxi Li, Ziyang Sony, and Bo Yang. TRACE: Learning 3d gaussian physical dynamics from multi-view videos. In *International Conference on Computer Vision*, 2025. 3
- [49] Shiqian Li, Ruihong Shen, Chi Zhang, and Yixin Zhu. Neural force field: Learning generalized physical representation from a few examples. *arXiv preprint arXiv:2502.08987*, 2025. 3
- [50] Zhengqi Li, Simon Niklaus, Noah Snavely, and Oliver Wang. Neural scene flow fields for space-time view synthesis of dynamic scenes. In *IEEE/CVF Conference on Computer Vision and Pattern Recognition*, 2021. 3

- [51] Zhengqi Li, Richard Tucker, Noah Snavely, and Aleksander Holynski. Generative image dynamics. In *IEEE/CVF Conference on Computer Vision and Pattern Recognition*, 2024. 3
- [52] Zhengqi Li, Richard Tucker, Forrester Cole, Qianqian Wang, Linyi Jin, Vickie Ye, Angjoo Kanazawa, Aleksander Holynski, and Noah Snavely. MegaSaM: Accurate, fast and robust structure and motion from casual dynamic videos. In *IEEE/CVF Conference on Computer Vision and Pattern Recognition*, 2025. 4
- [53] Zizhang Li, Hong-Xing Yu, Wei Liu, Yin Yang, Charles Herrmann, Gordon Wetzstein, and Jiajun Wu. WonderPlay: Dynamic 3d scene generation from a single image and actions. In *International Conference on Computer Vision*, 2025. 3
- [54] Jiajing Lin, Zhenzhong Wang, Shu Jiang, Yongjie Hou, and Min Jiang. Phys4DGen: A physics-driven framework for controllable and efficient 4d content generation from a single image. *arXiv preprint arXiv:2411.16800*, 2024. 3
- [55] Minghui Lin, Xiang Wang, Yishan Wang, Shu Wang, Fengqi Dai, Pengxiang Ding, Cunxiang Wang, Zhengrong Zuo, Nong Sang, Siteng Huang, and Donglin Wang. Exploring the evolution of physics cognition in video generation: A survey. *arXiv preprint arXiv:2503.21765*, 2025. 3
- [56] Daochang Liu, Junyu Zhang, Anh-Dung Dinh, Eunbyung Park, Shichao Zhang, and Chang Xu. Generative physical ai in vision: A survey, 2025. 3
- [57] Shaowei Liu, Zhongzheng Ren, Saurabh Gupta, and Shenglong Wang. PhysGen: Rigid-body physics-grounded image-to-video generation. In *European Conference on Computer Vision*, 2024. 3
- [58] Xinhang Liu, Yuxi Xiao, Donny Y. Chen, Jiashi Feng, Yu-Wing Tai, Chi-Keung Tang, and Bingyi Kang. Trace anything: Representing any video in 4d via trajectory fields. *arXiv preprint arXiv:2510.13802*, 2025. 3
- [59] Liying Lu, Ruizheng Wu, Huaijia Lin, Jiangbo Lu, , and Jiaya Jia. Video frame interpolation with transformer. In *IEEE/CVF Conference on Computer Vision and Pattern Recognition*, 2022. 1, 3
- [60] Michael Lutter, Christian Ritter, and Jan Peters. Deep lagrangian networks: Using physics as model prior for deep learning. In *International Conference on Learning Representations*, 2019. 3
- [61] Jiayi Lv, Yi Huang Huang, Mingfu Yan, Jiancheng Huang, Jianzhuang Liu, Yifan Liu Liu, Yafei Wen, Xiaoxin Chen, and Shifeng Chen. Gpt4motion: Scripting physical motions in text-to-video generation via blender-oriented gpt planning. In *IEEE/CVF Conference on Computer Vision and Pattern Recognition*, 2024. 3
- [62] Fanqing Meng, Jiaqi Liao, Xinyu Tan, Wenqi Shao, Quanfeng Lu, Kaipeng Zhang, Cheng Yu, Dianqi Li, Yu Qiao, and Ping Luo. Towards world simulator: Crafting physical commonsense-based benchmark for video generation. In *International Conference on Machine Learning*, 2025. 3
- [63] Ben Mildenhall, Pratul P. Srinivasan, Matthew Tancik, Jonathan T. Barron, Ravi Ramamoorthi, and Ren Ng. NeRF: Representing scenes as neural radiance fields for view synthesis. In *European Conference on Computer Vision*, 2020. 3
- [64] Saman Motamed, Laura Culp, Kevin Swersky, Priyank Jaini Jaini, and Robert Geirhos. Do generative video models understand physical principles?, 2025. 3
- [65] Xun Long Ng, Kian Eng Ong, Qichen Zheng, Yun Ni, Si Yong Yeo, and Jun Liu. Animal kingdom: A large and diverse dataset for animal behavior understanding. In *IEEE/CVF Conference on Computer Vision and Pattern Recognition*, 2022. 7, 1
- [66] Tuan Duc Ngo, Ashkan Mirzaei, Gordon Qian, Hanwen Liang, Chuang Gan, Evangelos Kalogerakis, Peter Wonka, and Chaoyang Wang. DELTA_v2: Dense efficient long-range 3d tracking for any video. *arXiv preprint arXiv:2508.01170*, 2025. 3
- [67] Tuan Duc Ngo, Peiye Zhuang, Chuang Gan, Evangelos Kalogerakis, Sergey Tulyakov, Hsin-Ying Lee, and Chaoyang Wang. DELTA: Dense efficient long-range 3d tracking for any video. In *International Conference on Learning Representations*, 2025. 3
- [68] Muyao Niu, Xiaodong Cun, Xintao Wang, Yong Zhang, Ying Shan, and Yinqiang Zheng. MOFA-Video: Controllable image animation via generative motion field adaptations in frozen image-to-video diffusion model. In *European Conference on Computer Vision*, 2024. 1, 3
- [69] NVIDIA. Cosmos world foundation model platform for physical ai. *arXiv preprint arXiv:2501.03575*, 2025. 1, 3, 7
- [70] OpenAI. Video generation models as world simulators. 1, 3
- [71] Karran Pandey, Matheus Gadelha, Yannick Hold-Geoffroy, Karan Singh, Niloy J. Mitra, and Paul Guerrero. Motion Modes: What could happen next? In *IEEE/CVF Conference on Computer Vision and Pattern Recognition*, 2025. 1, 3
- [72] William Peebles and Saining Xie. Scalable diffusion models with transformers. In *International Conference on Computer Vision*, 2023. 1, 3
- [73] F. Perazzi, J. Pont-Tuset, B. McWilliams, L. Van Gool, M. Gross, and A. Sorkine-Hornung. A benchmark dataset and evaluation methodology for video object segmentation. In *IEEE/CVF Conference on Computer Vision and Pattern Recognition*, 2016. 5, 1
- [74] Maziar Raissi, Paris Perdikaris, and George E Karniadakis. Physics-informed neural networks: A deep learning framework for solving forward and inverse problems involving nonlinear partial differential equations. *Journal of Computational Physics*, 2019. 3
- [75] Aditya Ramesh, Mikhail Pavlov, Gabriel Goh, Scott Gray, Chelsea Voss, Alec Radford, Mark Chen, and Ilya Sutskever. Zero-shot text-to-image generation. In *International Conference on Machine Learning*, 2021. 3
- [76] Fitsum Reda, Janne Kontkanen, Eric Tabellion, Deqing Sun, Caroline Pantofaru, and Brian Curless. FILM: Frame interpolation for large motion. In *European Conference on Computer Vision*, 2022. 1, 3
- [77] Robin Rombach, Andreas Blattmann, Dominik Lorenz, Patrick Esser, and Björn Ommer. High-resolution image

- synthesis with latent diffusion models. In *IEEE/CVF Conference on Computer Vision and Pattern Recognition*, pages 10674–10685, 2022. 3
- [78] Luca Savant Aira, Antonio Montanaro, Emanuele Aiello, Diego Valsesia, and Enrico Magli. MotionCraft: Physics-based zero-shot video generation. In *Advances in Neural Information Processing Systems*, 2024. 3
- [79] Daniel L. Schacter, Donna Rose Addis, and Randy L. Buckner. Remembering the past to imagine the future: the prospective brain. *Nature Reviews Neuroscience*, 2007. 1
- [80] Xiaoyu Shi, Zhaoyang Huang, Fu-Yun Wang, Weikang Bian, Dasong Li, Yi Zhang, Manyuan Zhang, Ka Chun Cheung, Simon See, Hongwei Qin, et al. Motion-i2v: Consistent and controllable image-to-video generation with explicit motion modeling. In *SIGGRAPH*, 2024. 1, 3
- [81] Hyeonjun Sim, Jihyong Oh, and Munchurl Kim. XVFI: extreme video frame interpolation. In *International Conference on Computer Vision*, 2021. 1, 3
- [82] Yang Song, Jascha Sohl-Dickstein, Diederik P Kingma, Abhishek Kumar, Stefano Ermon, and Ben Poole. Score-based generative modeling through stochastic differential equations. In *International Conference on Learning Representations*, 2021. 3
- [83] Xiyang Tan, Ying Jiang, Xuan Li, Zeshun Zong, Tianyi Xie, Yin Yang, and Chenfanfu Jiang. PhysMotion: Physics-grounded dynamics from a single image. *arXiv preprint arXiv:2411.17189*, 2024. 1, 3
- [84] Ilya Tolstikhin, Neil Houlsby, Alexander Kolesnikov, Lucas Beyer, Xiaohua Zhai, Thomas Unterthiner, Jessica Yung, Andreas Steiner, Daniel Keysers, Jakob Uszkoreit, Mario Lucic, and Alexey Dosovitskiy. MLP-Mixer: An all-mlp architecture for vision. *arXiv preprint arXiv:2105.01601*, 2021. 3
- [85] Basile Van Hoorick, Rundi Wu, Ege Ozguroglu, Kyle Sargent, Ruoshi Liu, Pavel Tokmakov, Achal Dave, Changxi Zheng, and Carl Vondrick. Generative camera dolly: Extreme monocular dynamic novel view synthesis. *European Conference on Computer Vision*, 2024. 7, 8
- [86] Ashish Vaswani, Noam Shazeer, Niki Parmar, Jakob Uszkoreit, Llion Jones, Aidan N. Gomez, Lukasz Kaiser, and Illia Polosukhin. Attention is all you need. In *Advances in Neural Information Processing Systems*, 2017. 3
- [87] Team Wan. Wan: Open and advanced large-scale video generative models. *arXiv preprint arXiv:2503.20314*, 2025. 1, 3, 7
- [88] Bo Wang, Jian Li, Yang Yu, Li Liu, Zhenping Sun, and Dewen Hu. SceneTracker: Long-term scene flow estimation network. *IEEE Transactions on Pattern Analysis and Machine Intelligence*, 2024. 3
- [89] Chaoyang Wang, Ben Eckart, Simon Lucey, and Orazio Gallo. Neural trajectory fields for dynamic novel view synthesis. *arXiv preprint arXiv: 2105.05994*, 2021. 3
- [90] Jiawei Wang, Liping Yuan, Yuchen Zhang, and Haomiao Sun. Tarsier: Recipes for training and evaluating large video description models. *arXiv preprint arXiv:2407.00634*, 2024. 5
- [91] Jing Wang, Ao Ma, Ke Cao, Jun Zheng, Zhanjie Zhang, Jiasong Feng, Shanyuan Liu, Yuhang Ma, Bo Cheng, Dawei Leng, Yuhui Yin, and Xiaodan Liang. WISA: World simulator assistant for physics-aware text-to-video generation. *arXiv preprint arXiv:2502.08153*, 2025. 3
- [92] Qianqian Wang, Yen-Yu Chang, Ruojin Cai, Zhengqi Li, Bharath Hariharan, Aleksander Holynski, and Noah Snavely. Tracking everything everywhere all at once. In *International Conference on Computer Vision*, 2023. 3
- [93] Qianqian Wang, Vickie Ye, Hang Gao, Weijia Zeng, Jake Austin, Zhengqi Li, and Angjoo Kanazawa. Shape of Motion: 4d reconstruction from a single video. In *International Conference on Computer Vision*, 2025. 3, 4, 7, 8
- [94] Xiaojuan Wang, Boyang Zhou, Brian Curless, Ira Kemelmacher-Shlizerman, Aleksander Holynski, and Steven M Seitz. Generative inbetweening: Adapting image-to-video models for keyframe interpolation. In *International Conference on Learning Representations*, 2025. 1, 3
- [95] Nicholas Watters, Daniel Zoran, Theophane Weber, Peter Battaglia, Razvan Pascanu, and Andrea Tacchetti. Visual interaction networks: Learning a physics simulator from video. In *Advances in Neural Information Processing Systems*, 2017. 3
- [96] Thaddäus Wiedemer, Yuxuan Li, Paul Vicol, Shixiang Shane Gu, Nick Matarese, Kevin Swersky, Been Kim, Priyank Jaini, and Robert Geirhos. Video models are zero-shot learners and reasoners. *arXiv preprint arXiv:2509.20328*, 2025. 5
- [97] Guanjun Wu, Taoran Yi, Jiemin Fang, Lingxi Xie, Xiaopeng Zhang, Wei Wei, Wenyu Liu, Qi Tian, and Xinggang Wang. 4d gaussian splatting for real-time dynamic scene rendering. In *IEEE/CVF Conference on Computer Vision and Pattern Recognition*, 2024. 3
- [98] Jiajun Wu, Ilker Yildirim, Joseph J. Lim, William T. Freeman, , and Joshua B. Tenenbaum. Galileo: Perceiving physical object properties by integrating a physics engine with deep learning. In *Advances in Neural Information Processing Systems*, 2015. 3
- [99] Jiajun Wu, Erika Lu, Pushmeet Kohli, Bill Freeman, and Josh Tenenbaum. Learning to see physics via visual deanimation. In *Advances in Neural Information Processing Systems*, 2017. 3
- [100] Wenqi Xian, Jia-Bin Huang, Johannes Kopf, and Changil Kim. Space-time neural irradiance fields for free-viewpoint video. In *IEEE/CVF Conference on Computer Vision and Pattern Recognition*, 2021. 3
- [101] Yuxi Xiao, Qianqian Wang, Shangzhan Zhang, Nan Xue, Sida Peng, Yujun Shen, and Xiaowei Zhou. SpatialTracker: Tracking any 2d pixels in 3d space. In *IEEE/CVF Conference on Computer Vision and Pattern Recognition*, 2024. 3
- [102] Yuxi Xiao, Jianyuan Wang, Nan Xue, Nikita Karaev, Iurii Makarov, Bingyi Kang, Xin Zhu, Hujun Bao, Yujun Shen, and Xiaowei Zhou. SpatialTrackerV2: 3d point tracking made easy. In *IEEE/CVF International Conference on Computer Vision*, 2025. 3
- [103] Tianyi Xie, Zeshun Zong, Yuxing Qiu, Xuan Li, Yutao Feng, Yin Yang, and Chenfanfu Jiang. PhysGaussian: Physics-integrated 3d gaussians for generative dynamics.

- In *IEEE/CVF Conference on Computer Vision and Pattern Recognition*, 2024. 3
- [104] Tianyi Xie, Yiwei Zhao, Ying Jiang, and Chenfanfu Jiang. PhysAnimator: Physics-guided generative cartoon animation. In *IEEE/CVF Conference on Computer Vision and Pattern Recognition*, 2025. 1, 3
- [105] Tianshuo Xu, Zhifei Chen, Leyi Wu, Hao Lu, Yuying Chen, Lihui Jiang, Bingbing Liu, and Yingcong Chen. Motion Dreamer: Realizing physically coherent video generation through scene-aware motion reasoning. *arXiv preprint arXiv:2412.00547*, 2024. 3
- [106] Qiyao Xue, Xiangyu Yin, Boyuan Yang, and Wei Gao. PhyT2V: Llm-guided iterative self-refinement for physics-grounded text-to-video generation. In *IEEE/CVF Conference on Computer Vision and Pattern Recognition*, 2025. 3
- [107] Jinyu Yang, Mingqi Gao, Zhe Li, Shang Gao, Fangjing Wang, and Feng Zheng. Track Anything: Segment anything meets videos, 2023. 4
- [108] Xindi Yang, Baolu Li, Yiming Zhang, Zhenfei Yin, Lei Bai, Liqian Ma, Zhiyong Wang, Jianfei Cai, Tien-Tsin Wong, Huchuan Lu, and Xu Jia. VLIPP: Towards physically plausible video generation with vision and language informed physical prior. In *International Conference on Computer Vision*, 2025. 3
- [109] Ziyi Yang, Xinyu Gao, Wen Zhou, Shaohui Jiao, Yuqing Zhang, and Xiaogang Jin. Deformable 3d gaussians for high-fidelity monocular dynamic scene reconstruction. *IEEE/CVF Conference on Computer Vision and Pattern Recognition*, 2024. 3
- [110] Zeyu Yang, Hongye Yang, Zijie Pan, and Li Zhang. Real-time photorealistic dynamic scene representation and rendering with 4d gaussian splatting. In *International Conference on Learning Representations*, 2024. 3
- [111] Zhuoyi Yang, Jiayan Teng, Wendi Zheng, Ming Ding, Shiyu Huang, Jiazheng Xu, Yuanming Yang, Wenyi Hong, Xiaohan Zhang, Guanyu Feng, et al. CogVideoX: Text-to-video diffusion models with an expert transformer. In *International Conference on Learning Representations*, 2025. 1, 3
- [112] Ye Yuan, Jiaming Song, Umar Iqbal, Arash Vahdat, and Jan Kautz. Physdiff: Physics-guided human motion diffusion model. In *International Conference on Computer Vision*, 2023. 3
- [113] Yu Yuan, Xijun Wang, Yichen Sheng, Prateek Chennuri, Xingguang Zhang, and Stanley Chan. Generative Photography: Scene-consistent camera control for realistic text-to-image synthesis. *IEEE/CVF Conference on Computer Vision and Pattern Recognition*, 2025. 3, 7
- [114] Yu Yuan, Xijun Wang, Tharindu Wickremasinghe, Zeeshan Nadir, Bole Ma, and Stanley H. Chan. NewtonGen: Physics-consistent and controllable text-to-video generation via neural newtonian dynamics. *arXiv preprint arXiv: 2509.21309*, 2025. 1, 3
- [115] Chenyu Zhang, Daniil Cherniavskii, Andrii Zadaianchuk, Antonios Tragoudaras, Antonios Vozikis, Thijmen Nijdam, Derck W. E. Prinzhorn, Mark Bodracska, Nicu Sebe, and Efstratios Gavves. Morpheus: Benchmarking physical reasoning of video generative models with real physical experiments. *arXiv preprint arXiv:2504.02918*, 2025. 3
- [116] Ke Zhang, Cihan Xiao, Yiqun Mei, Jiacong Xu, and Vishal M. Patel. Think before you diffuse: Lms-guided physics-aware video generation. *arXiv preprint arXiv:2505.21653*, 2025. 3
- [117] Mingtong Zhang, Kaifeng Zhang, and Yunzhu Li. Dynamic 3d gaussian tracking for graph-based neural dynamics modeling. In *8th Annual Conference on Robot Learning*, 2024. 3
- [118] Richard Zhang, Phillip Isola, Alexei A Efros, Eli Shechtman, and Oliver Wang. The unreasonable effectiveness of deep features as a perceptual metric. In *IEEE/CVF Conference on Computer Vision and Pattern Recognition*, 2018. 7
- [119] Tianyuan Zhang, Hong-Xing Yu, Rundi Wu, Brandon Y. Feng, Changxi Zheng, Noah Snively, Jiajun Wu, and William T. Freeman. PhysDreamer: Physics-based interaction with 3d objects via video generation. In *European Conference on Computer Vision*, 2024. 3
- [120] Xiangdong Zhang, Jiaqi Liao, Shaofeng Zhang, Fanqing Meng, Xiangpeng Wan, Junchi Yan, and Yu Cheng. VideoREPA: Learning physics for video generation through relational alignment with foundation models. *arXiv preprint arXiv:2505.23656*, 2025. 3
- [121] Yiqi Zhong, Luming Liang, Ilya Zharkov, and Ulrich Neumann. Mmvp: Motion-matrix-based video prediction. In *International Conference on Computer Vision*, 2023. 1, 3
- [122] Yiqi Zhong, Luming Liang, Bohan Tang, Ilya Zharkov, and Ulrich Neumann. Motion graph unleashed: A novel approach to video prediction. In *Advances in Neural Information Processing Systems*, 2024. 1, 3
- [123] Yaofeng Desmond Zhong and Naomi Ehrich Leonard. Un-supervised learning of lagrangian dynamics from images for prediction and control. In *Advances in Neural Information Processing Systems*, 2020. 3
- [124] Zhihang Zhong, Gurunandan Krishnan, Xiao Sun, Yu Qiao, Sizhuo Ma, and Jian Wang. Clearer frames, anytime: Resolving velocity ambiguity in video frame interpolation. In *European Conference on Computer Vision*, 2024. 1, 3, 7
- [125] Gaoyue Zhou, Hengkai Pan, Yann Lecun, and Lerrel Pinto. DINO-WM: World models on pre-trained visual features enable zero-shot planning. *arXiv preprint arXiv: 2411.04983*, 2024. 1, 3

SeeU: Seeing the Unseen World via 4D Dynamics-aware Generation

Supplementary Material

7. Introduction

This supplementary material provides additional discussions and details on the SeeU45 data (Section 8), Continuous 4D Dynamics Model (C4DD) design and ablation study (Section 9), spatial-temporal in-context generation (Section 10), the 3D geometric metrics used in the experiments (Section 11), the limitations (Section 12), and more visual results (Section 13).

To more clearly demonstrate SeeU’s temporal and spatial generation abilities, we recommend that readers refer to the **videos** included in the Project Page at <https://yuyuanspace.com/SeeU/>.

8. More Details of SeeU45 Data

The SeeU45 dataset consists of 45 dynamic scenes, including 10 scenes that we manually captured and 35 scenes collected from public video datasets [11, 17, 19, 65, 73]. Each scene is provided in two forms: a ground-truth (GT) sequence and a training subset. The GT split contains the full dynamic sequence for each scene, while the training split is constructed by taking either the middle segment of the GT sequence or a temporally sampled version of that middle segment.

SeeU45 covers a diverse set of conditions in terms of scene type, foreground subjects, camera regimes, and motion types. A summary of the dataset statistics is provided in Table 4.

9. More Details of Continuous 4D Dynamics Model

9.1. Architecture.

In Algorithm 1 we present the detailed architecture of the Continuous 4D Dynamics Model (C4DD). During training, C4DD learns continuous and smooth motion/camera bases by optimizing B-spline control points, and enforces physically consistent and smooth extrapolation through physics-aware constraints.

9.2. More Details About Ablation Study on C4DD Architecture.

To assess the necessity of the proposed C4DD architecture, we replace the B-spline-based design with a pure MLP layer and train it thoroughly. As shown in Fig. 7, although the MLP-based variant can roughly fit the overall trend of the motion bases, the resulting continuous trajectories are highly noisy and lack smoothness. This significantly degrades the

Composition	
Scenes (total)	45
Our captured	10
From public datasets	35
Scene Types	
Indoor scenes	6
Outdoor scenes	39
Foreground Subjects (some scenes contain both)	
Humans	8
Animals	13
Robots	3
Vehicles	18
Everyday objects	12
Camera Regimes	
Static	10
Handheld	28
Drone	7
Motion Types	
Rigid motion	21
Non-rigid motion	24
Frame Statistics	
GT frames / scene (min / max / avg)	9 / 521 / 80.24
Train frames / scene (min / max / avg)	7 / 47 / 15.96

Table 4. Statistics of the SeeU45 dataset.

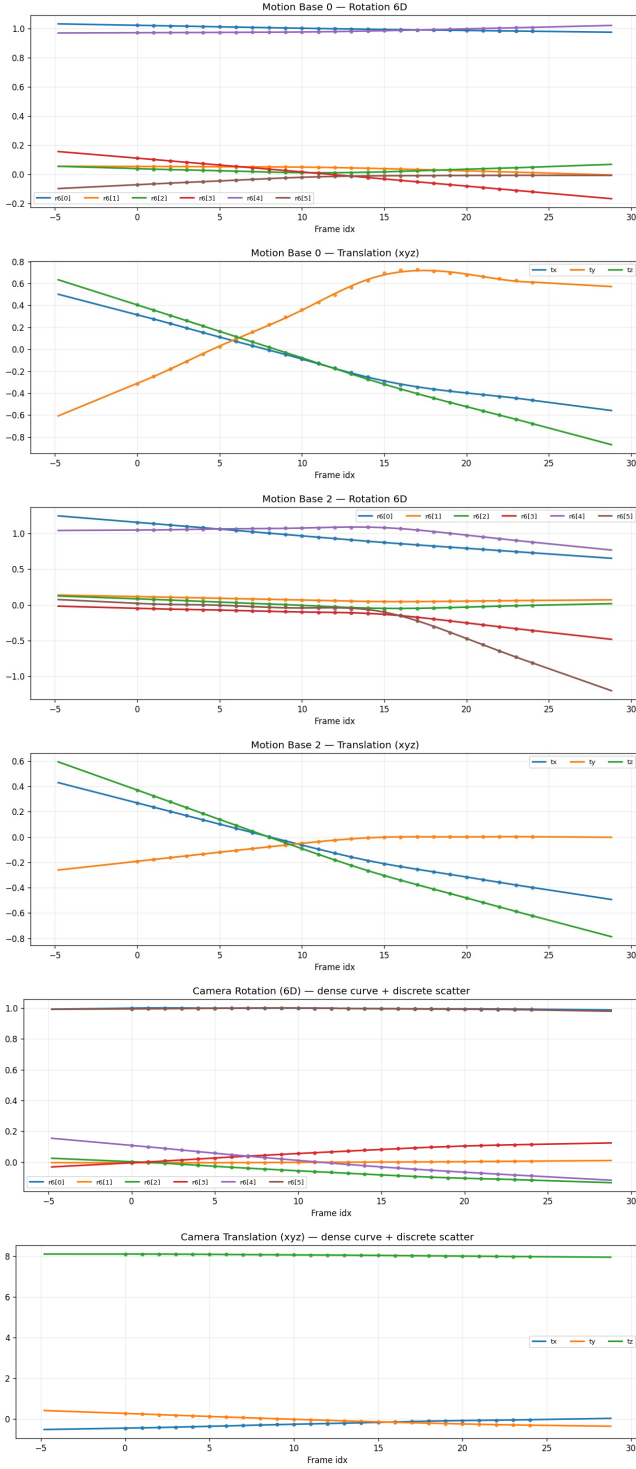
spatio-temporal quality of the model’s predictions (see Fig. 8).

10. More Details of Spatial-Temporal In-Context Generation

The third stage, context-aware video filling, is mainly adapted from VACE [38]. During inference, We provide three types of contextual information:

1. **Text prompt.** The text prompt describes the global spatio-temporal semantics, adds extra guidance for the regions to be filled, and emphasizes physical consistency in the scene. For example: “A camel is walking slowly in his enclosure. The enclosure has sand on the floor, surrounded by a wooden fence and planks. The background has trees. Restore the masked regions of the video with the background of the enclosure. Make the colors and background behind the camel realistic and continuous.”
2. **Projected frames.** These frames come from our 4D →

(a) C4DD (B-spline-based)



(b) C4DD (MLP-based)

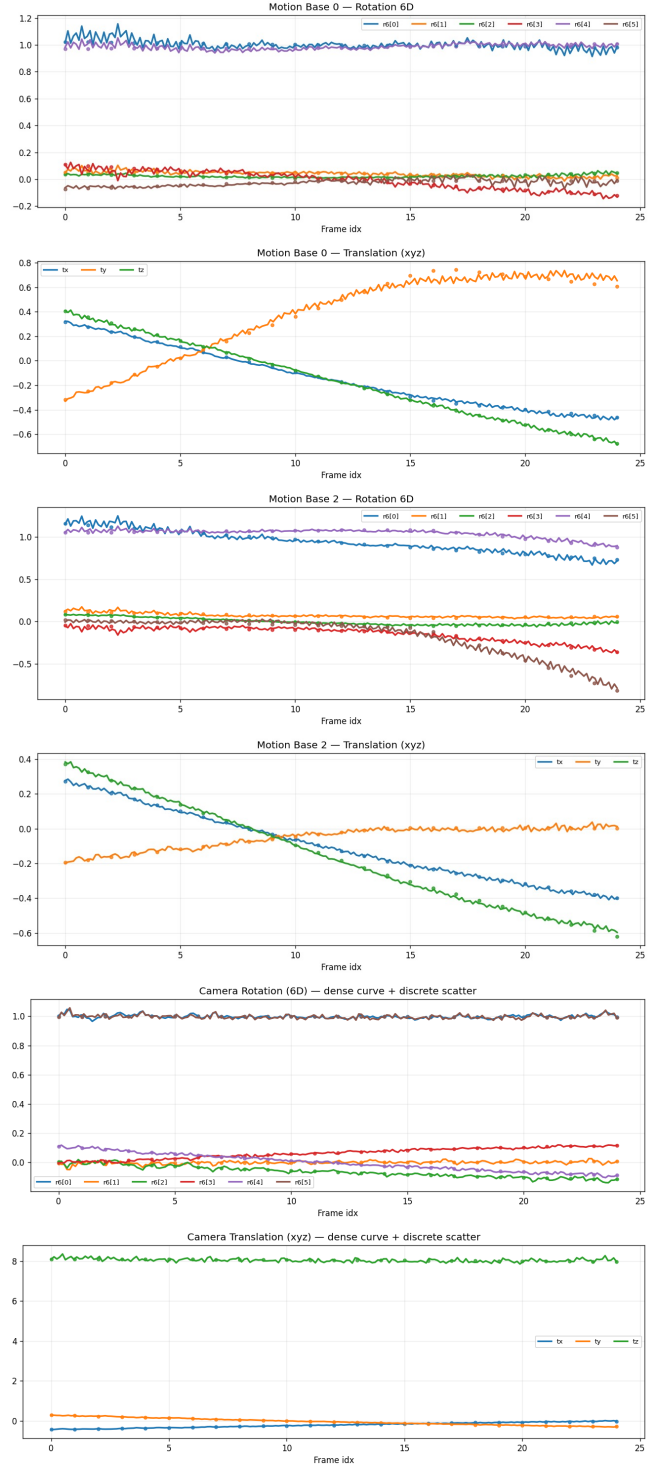


Figure 7. The C4DD with MLP variant (b) predicts motion bases with reduced temporal smoothness and physical consistency, confirming the advantageous inductive bias of spline priors (a) for continuous dynamics.

Algorithm 1 Continuous 4D Dynamics Model Architecture

Require: Number of motion bases K , number of control points M , degree p .

```

1: Initialization:
2: Build an open-uniform knot vector  $\{u_i\}_{i=0}^{M+p}$  on  $[0, 1]$ .
3: Initialize motion control points  $\mathbf{C}^{\text{mot}} \in \mathbb{R}^{K \times 9 \times M}$ .
4: Initialize camera control points  $\mathbf{C}^{\text{cam}} \in \mathbb{R}^{1 \times 9 \times M}$ .

5: function BSPLINEBASIS( $\mathbf{t}_{01}$ )  $\triangleright \mathbf{t}_{01} \in (0, 1)^{B \times 1}$ 
6:   Compute B-spline basis  $\mathbf{B} \in \mathbb{R}^{B \times M}$  using Cox-de
   Boor recursion on knots  $\{u_i\}$ .
7:   return  $\mathbf{B}$ 
8: end function

9: function FORWARD( $\mathbf{t}_{\text{norm}}$ )  $\triangleright \mathbf{t}_{\text{norm}} \in [-1, 1]^{B \times 1}$ 
10:  Map time to  $(0, 1)$ :  $\mathbf{t}_{01} \leftarrow \text{clip}(0.5 \mathbf{t}_{\text{norm}} +$ 
    $0.5, 10^{-6}, 1 - 10^{-6})$ .
11:   $\mathbf{B} \leftarrow \text{BSPLINEBASIS}(\mathbf{t}_{01})$   $\triangleright \mathbf{B} \in \mathbb{R}^{B \times M}$ 
12:  Motion bases:  $\mathbf{Y}^{\text{mot}} \leftarrow \mathbf{C}^{\text{mot}} \mathbf{B}^T \in \mathbb{R}^{K \times 9 \times B}$ .
13:  Camera pose:  $\mathbf{Y}^{\text{cam}} \leftarrow \mathbf{C}^{\text{cam}} \mathbf{B}^T \in \mathbb{R}^{1 \times 9 \times B}$ .
14:  Reshape to  $\mathbf{Y}^{\text{mot}} \in \mathbb{R}^{K \times B \times 9}$ ,  $\mathbf{Y}^{\text{cam}} \in \mathbb{R}^{B \times 9}$ .
15:  return  $\mathbf{Y}^{\text{mot}}$ ,  $\mathbf{Y}^{\text{cam}}$ 
16: end function

17: function FORWARDEXTRAP( $\mathbf{t}_{\text{norm}}$ )  $\triangleright$  linear
   extrapolation outside  $[-1, 1]$ 
18:   $\mathbf{t}_{\text{clamp}} \leftarrow \text{clip}(\mathbf{t}_{\text{norm}}, -1, 1)$ 
19:   $\mathbf{Y}_0^{\text{mot}}, \mathbf{Y}_0^{\text{cam}} \leftarrow \text{FORWARD}(\mathbf{t}_{\text{clamp}})$ 
20:  Estimate endpoint slopes  $\mathbf{s}_L, \mathbf{s}_R$  at  $t = -1$  and  $t = 1$ 
   using finite differences (step size  $\Delta t \approx 2/(T - 1)$ ).
21:  Initialize  $\mathbf{Y}^{\text{mot}} \leftarrow \mathbf{Y}_0^{\text{mot}}$ ,  $\mathbf{Y}^{\text{cam}} \leftarrow \mathbf{Y}_0^{\text{cam}}$ .
22:  for each time index  $b$  do
23:    if  $t_{\text{norm}}[b] < -1$  then
24:       $\Delta t \leftarrow t_{\text{norm}}[b] + 1$ 
25:      Extrapolate  $\mathbf{Y}^{\text{mot}}[:, b, :]$  and  $\mathbf{Y}^{\text{cam}}[b, :]$  us-
   ing left endpoint and slope  $\mathbf{s}_L$ .
26:    else if  $t_{\text{norm}}[b] > 1$  then
27:       $\Delta t \leftarrow t_{\text{norm}}[b] - 1$ 
28:      Extrapolate  $\mathbf{Y}^{\text{mot}}[:, b, :]$  and  $\mathbf{Y}^{\text{cam}}[b, :]$  us-
   ing right endpoint and slope  $\mathbf{s}_R$ .
29:    end if
30:  end for
31:  return  $\mathbf{Y}^{\text{mot}}$ ,  $\mathbf{Y}^{\text{cam}}$ 
32: end function

```

2D rendering. Pixels in the inpainting masks (defined below) are set to a constant gray value (127), so that the projected frames act as a structural scaffold for the video while clearly indicating where content to be synthesized.

3. **Inpainting masks.** The masks specify the unseen regions that need to be filled. They are constructed from

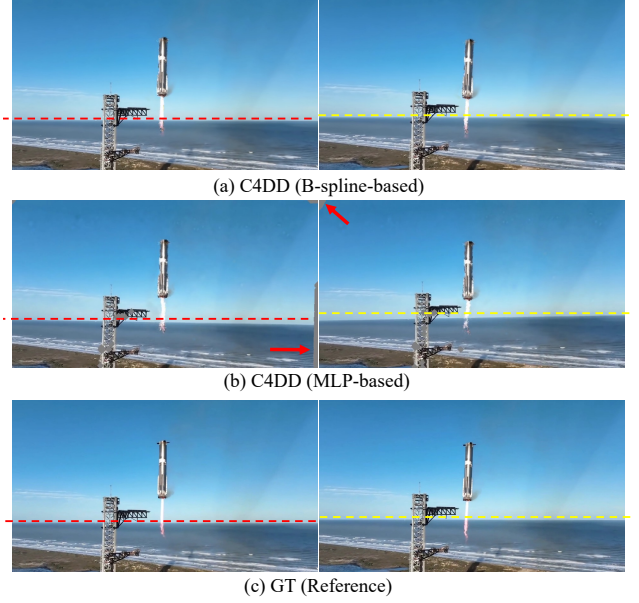


Figure 8. Visual comparison on C4DD Architectures. The C4DD with spline constrains (a) has better smoothness and physical consistency (both camera pose and foreground dynamics).

three types of areas: (1) regions that are never observed (novel viewpoints or previously occluded areas), which are naturally identified through the inverse-projection process; (2) locations where the projected Gaussians have low confidence, detected via a threshold on the opacity values; and (3) thin structures and sharp depth discontinuities that may cause projection artifacts (e.g., along object boundaries and occlusion edges), detected by checking whether the relative depth difference exceeds a predefined threshold.

11. More Details of Proposed Metrics

To evaluate the spatial consistency of generated videos in unseen viewpoints, we adopt two standard two-view geometric metrics: *Epipolar Error (EE)* and *Epipolar Inlier Ratio (EIR)*. These metrics quantify how well the generated frames obey the underlying epipolar geometry defined by a fundamental matrix estimated from visual correspondences.

Setup. Given a reference frame I_1 and a generated frame I_2 , we extract putative feature correspondences $\{(x_1^{(i)}, x_2^{(i)})\}_{i=1}^N$ using SIFT with cross-check and ratio test. The fundamental matrix F is then estimated via RANSAC:

$$F = \arg \min_{F'} \sum_{i \in \mathcal{I}(F')} \text{EE}(x_1^{(i)}, x_2^{(i)}, F'), \quad (8)$$

where $\mathcal{I}(F')$ denotes the RANSAC inlier set.

Epipolar Error (EE). For a correspondence (x_1, x_2) with

homogeneous coordinates $\tilde{x}_1 = (x_1^\top, 1)^\top$ and $\tilde{x}_2 = (x_2^\top, 1)^\top$, the epipolar constraint states:

$$\tilde{x}_2^\top F \tilde{x}_1 = 0. \quad (9)$$

Deviations from this constraint reflect geometric inconsistency. We adopt the *Sampson approximation* of the re-projection error:

$$EE(x_1, x_2; F) = \sqrt{\frac{(\tilde{x}_2^\top F \tilde{x}_1)^2}{(F \tilde{x}_1)_0^2 + (F \tilde{x}_1)_1^2 + (F^\top \tilde{x}_2)_0^2 + (F^\top \tilde{x}_2)_1^2}}. \quad (10)$$

This metric has several desirable properties:

- It is expressed in pixel units and directly interpretable.
- It approximates the *geometric reprojection error* without requiring camera intrinsics.
- It is robust to scale ambiguity inherent to fundamental matrices.

In practice, we report:

$$EE_{\text{median}} = \text{median}_{I \in \mathcal{I}(F)} EE(x_1^{(i)}, x_2^{(i)}; F),$$

where a lower value indicates better geometric alignment between the generated view and the reference view.

Epipolar Inlier Ratio (EIR). While EE measures the *accuracy* of the geometric alignment, we also evaluate the *stability* of the geometry via an inlier ratio:

$$EIR = \frac{|\mathcal{I}(F)|}{N}, \quad (11)$$

where N is the total number of matched correspondences before RANSAC. A higher EIR indicates that a larger portion of correspondences can be explained by a valid two-view geometry, suggesting more realistic spatial structure in the generated frame.

EIR is particularly informative in generative settings because:

- generated videos may contain distortions that destroy epipolar geometry,
- RANSAC tends to reject correspondences that violate 3D plausibility,
- a low EIR implies strong geometric hallucination or temporal drift.

Together, EE and EIR evaluate the spatial fidelity of generated videos:

- **EE** reflects how close the video is to a physically plausible two-view geometry.
- **EIR** reflects how consistently the generator maintains global 3D structure.

Both metrics do not require camera intrinsics and thus can be applied to arbitrary videos, making them suitable for evaluating geometry realism in this work.

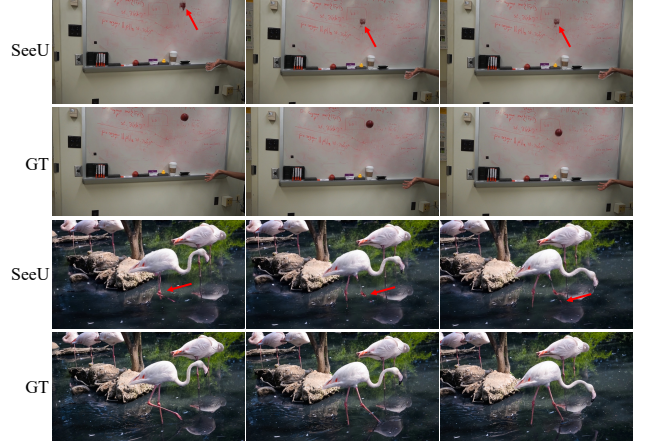


Figure 9. SeeU’s performance degrades on inputs containing thin structures or lacking texture, reflecting the inherent limitations of existing base models.

12. Limitations

In the first-stage 2D-4D lifting, the performance of SeeU is strongly constrained by the quality of the upstream geometry modules, including camera pose estimation, tracking, and depth prediction. As a result, SeeU requires input videos with salient foreground objects and sufficient spatial details.

As shown in Fig. 9, when the foreground is extremely small or lacks rich texture, these modules become unreliable and the final outputs degrade accordingly. We illustrate such failure cases on small or low-texture foregrounds in the examples below.

13. More Visual Results

We encourage readers to directly watch the **videos** provided in the project page, as they best demonstrate the temporal and spatial behaviors of our method. For completeness, we also include a few representative visual examples below (Fig. 10 to Fig. 12) as a preview.



Input Frames



Visualization of the Learned Continuous Dynamics



Past Frames by SeeU



In-Between Frames by SeeU

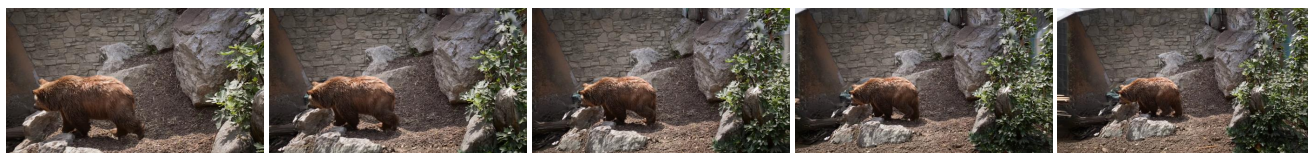


Future Frames by SeeU

Figure 10. Unseen Temporal World Generated by SeeU.



Input Frames



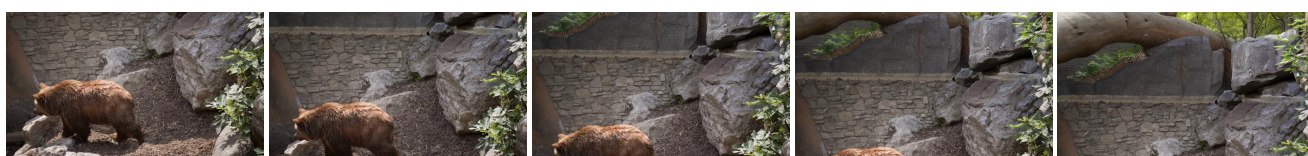
Dolly Out by SeeU



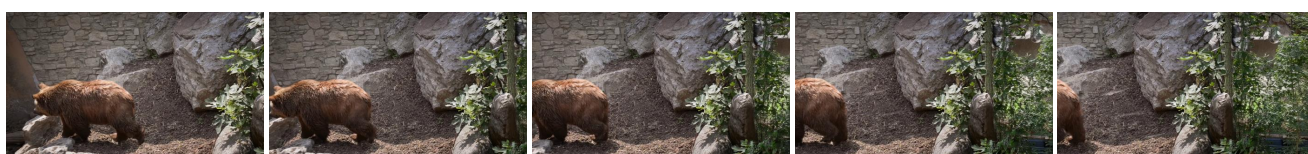
Dolly Left by SeeU



Dolly Up by SeeU



Tilt Up by SeeU



Pan Right by SeeU

Figure 11. Unseen Spatial World Generated by SeeU.



Input Frames



Object Removal by SeeU



Input Frames



Object Replacement by SeeU



Input Frames



Time Lapse by SeeU

Figure 12. Videos edited by SeeU.